Mechanics of Materials 159 (2021) 103903

Contents lists available at ScienceDirect

Mechanics of Materials

journal homepage: www.elsevier.com/locate/mechmat

Focus on the deformation mechanism at the interfacial layer in nano-reinforced polymers: A molecular dynamics study of silica - poly (methyl methacrylate) nano-composite

Fahmi Bedoui [a,b,*], Andres Jaramillo-Botero [b], Tod A. Pascal [c], William A. Goddard III [b]

[a] Roberval FRE-CNRS 2012, Sorbonne Universités, Université de Technologie de Compiègne, France
[b] Materials and Process Simulation Center, California Institute of Technology, Pasadena, CA, USA
[c] Materials Science and Engineering and the Sustainable Power and Energy Center, University of California San Diego, La Jolla, CA, USA

ARTICLE INFO

Keywords:
Size effect
Interfacial deformation mechanism
Molecular dynamics
2-PT method

ABSTRACT

The effects of nanoparticle size on the "macroscopic" mechanical response and interfacial interaction in the case of model nano-reinforced polymers were investigated using molecular dynamics simulations. Different ensembles, of homogeneous polymer matrices, amorphous silica particle, and their binary mixtures were prepared. The binary mixture was made with silica nano-particle 3 nm in size, embedded in poly (methyl methacrylate) or PMMA polymeric matrix. At the macroscopic scale, the mechanical response of the matrix and nano-composite was evaluated using simulated tensile tests. Interfacial interaction between the NP and the PMMA matrix was qualitatively evaluated using the thermodynamic analysis of nanocomposite systems. Entropy (S) and internal energy (E) were derived from relatively short molecular dynamics trajectories, using the two-phase thermodynamic method (2-PT). The PMMA matrix was decomposed into concentric layers composed of atoms from different polymer chains but located at an equal distance from the center of mass of the silica NP. For both nanocomposite systems, the interface layer of the polymer closest to the silica NP surface exhibited both the lowest entropy and a well-organized structure. Entropy and internal energy patterns were derived from tensile stretched samples. Entropy and internal energy variation on stretched samples revealed the existence of two distinct domains. The first domain deformation was a mixture of internal energy increase and entropy decrease. In the second domain, the deformation mechanism was mostly governed by variations in entropy. These observations will be discussed about polymer – nanoparticle attractivity.

1. Introduction

Nano-reinforced materials, particularly polymers, have received significant attention in recent decades, in industry, research, and academia. Nano-scale fillers can offer a range of features (nature, shape, and concentration) to modify/enhance the properties of polymer matrices. The mechanical, thermal, etc. properties of nanocomposites have been widely investigated. Experimental data obtained recently on nano-reinforced materials revealed that various properties, in particular mechanical, depend on the size of the used nanoparticle (NP) (Bliviet al., 2016; Blivi et al., 2020). Similarly, block copolymers made of covalently-bonded stiff and soft blocks also revealed elastic properties that depend on soft or stiff block size within the polymeric chains (Bedoui et al., 2012). These two examples evidenced the fact that in heterogeneous materials in general, and nano-reinforced polymers in particular, macroscopic properties do not only depend on the volume fraction and heterogeneity shape ratio, but also the size of the heterogeneous species at the nanoscale. Size dependency, shape ratio, and volume fraction add to the design space of nano-reinforced polymeric materials. Previously developed micromechanical models that described nanoscale interactions were based on the Eshelby assumption (Eshelby, 1957) that only the shape ratio and volume fraction play a part in the overall mechanical response of the materials being studied. New experimental results (Bliviet al., 2016; Bedoui et al., 2012) demonstrate that such models were unable to handle the dependency of a materials' macroscopic response on the size of the reinforcing nano-particles. To overcome this limitation, new approaches have emerged in the literature (Marcadon et al., 2007; Brisard et al., 2010; Dormieux and Kondo, 2013;

* Corresponding author. Roberval FRE-CNRS 2012, Sorbonne Universités, Université de Technologie de Compiègne, France.
E-mail addresses: fahmi.bedoui@utc.fr, fbedoui@wag.caltech.edu, bedoui@gmail.com (F. Bedoui).

https://doi.org/10.1016/j.mechmat.2021.103903
Received 4 February 2021; Received in revised form 4 May 2021; Accepted 5 May 2021
Available online 8 May 2021

Yvonnet et al., 2008; Ronald and Vijay, 2000). One such approach expresses the effect of particle size by introducing a third material phase, such as a polymeric layer around the nano-particles with different elastic properties to the polymeric matrix (Marcadon et al., 2007). The mechanical properties of this new material layer were inaccessible to the experimental techniques used in material characterization. The macroscopic response of the materials was thus deduced based on *a posteriori* calibration of the interfacial properties (layer thickness and mechanical properties). The introduction of an interphase layer surrounding the nano-particle enhanced the ability of previous micromechanical-based models to handle size distribution dependency (Diani and Gilormini, 2014). As such, they could be used to explore and understand the mechanical response of nano-reinforced polymers without necessarily being predictive. In a second approach, the effect of particle size was expressed through interfacial stress discontinuity (Brisard et al., 2010; Dormieux and Kondo, 2013) using the Young-Laplace equation. As such, excess stress at the interface was introduced into the models through two elastic-like parameters (bulk and shear surface properties) (Yvonnet et al., 2008). It is worth noting that in this method, the elastic-like parameters were not deduced on the polymeric interface but rather on the nano-particle surface (Ronald and Vijay, 2000). For this reason, these parameters do not account for the interaction between the polymer and the nanoparticle.

Both approaches incorporated the effect of particle size, even though the parameters used were not identified as *"a priori"*. This is mostly due to the difficulties associated with quantitatively describing the physical and mechanical mechanisms involved in the nanoparticle-polymeric matrix interaction. Particle-matrix interaction in the case of nanoparticle-based reinforced polymers has been the focus of intense research activities in recent years (Rittigstein et al., 2007; Brown et al., 2008; Berriot et al., 2002). Understanding the nature of the interactions at that level is required to help predict the macroscopic response of such materials. At the physicochemical level, the polymer-nanoparticle interaction has also been studied thoroughly recently (Rittigstein et al., 2007; Brown et al., 2008; Berriot et al., 2002; Papon et al., 2011, 2012; Schadler, 2007; Chevigny et al., 2011). However, these studies target large length scales that include the interface and bulk regions. As such, the derived physical parameters represent the averaged response (homogenization) of a larger zone composed of different materials, from which it is not possible to extract the interfacial response. Therefore, the contribution of the interface or third phase layer could be neither identified nor quantified. This lack of precision has hampered the development of mechanical models capable of accurately describing the interaction mechanisms between nanoparticles and the surrounding polymeric matrix.

Given the limitations encountered in the micromechanical continuum-level modeling and the experimental characterization of such materials, atomistic tools appear to be the most adequate alternative, as they offer the possibility of probing and connecting the different hierarchical structures involved, from the atomic to the engineering scale. In their work on carbon nano-tube (CNT) reinforced PMMA Arash et al. (2014) thoroughly explored the interactions between CNT and polymeric matrix and the dependency of the overall mechanical response on the size of the CNT. Such dependency was introduced into micromechanical models through polymeric layers around the CNT with its elastic properties. The elastic properties were derived from the interaction energy between the CNT and poly (methyl methacrylate) - PMMA. This energy was defined through the cut-off parameter of the force field used; for this reason, the elastic properties identified represented the properties not only of the interface but also of the mixture of the interface and the polymeric materials within the cut-off parameter. Nevertheless, the use of "third phase" elastic properties within an appropriate micromechanical model was shown to enhance the predicted results. In more recent data, size effects on the effective strength of nanocomposite materials were investigated (Lucchetta et al., 2021). Molecular dynamics tools were used to understand the influence of the inclusiuoin size on the materials behavior. From this work author concluded that interfacial interactions are size dependent (Lucchetta et al., 2021).

In this work, we explore size effects with smaller particle sizes than reported in the literature (Bliviet al., 2016), using particle diameters of 3 nm. The overall mechanical response was then correlated to local thermodynamics properties (Lin et al., 2003, 2010; Pascal and Lin, 2011), which allowed us to shed light on the fundamental mechanisms responsible for the size-induced enhancement in the mechanical response of nano-reinforced polymeric materials.

2. Materials and methods

Model nanocomposites were prepared with binary mixtures of silica nanoparticles and a PMMA matrix. Specifically, a silica nanoparticle of 3 nm in size was embedded into a PMMA matrix, made of ten and twenty chains, respectively, and each chain composed of two hundred monomers. The PMMA chain was built using the polymer builder package in the Schrodinger Maestro tool (Matestro, 2018). An atactic configuration was chosen with random backbone dihedral distribution, as this allows for a more accurate representation of the real polymer conformation. The silica particle was prepared and cut from a cristobalite supercell (Pedone et al., 2008) as presented in Fig. 1. The preparation protocol included heating the bulk supercell to 5000 K for 20 ps and cooling from 5000 K to 300 K, with isothermal control at intermediate temperatures (3000, 2000, 1500, 1000, 900, 500 K) for 20 ps to obtain amorphous silica (validated against experimental densities between 1.9 and 2.2 g/cc). Spherical nanoparticles were then cut using Schrodinger's Maestro building tools (Matestro, 2018).

The silica surface was then hydrogen-terminated to avoid any erroneous coordination of the surface oxygen atoms. Packmol (Martínez and Martínez, 2003; Martínez et al., 2009) software was used to pack the polymeric chains around the silica particle (Fig. 2) at a constant volume fraction of 5.21%. The model structures obtained were then formatted into a LAMMPS data file. The binary system was characterized using a DREIDING (Mayo et al., 1990) force field under the LAMMPS (http://lammps.san; Plimpton, 1995) molecular dynamics platform. The use of the DREIDING force field was motivated by two points: i) the availability of established parameters for modeling silica and PMMA polymers and ii) the computational efficiency one can find in fixed-charge simulations of molecular systems. The DREIDING force field accounts for interactions from bond stretching, changes in bond angle and dihedral rotation, and van der Waals and electrostatics non-bonded interactions. To account for the possible hydrogen bonding interaction between the silica and polymeric chains, the hydrogen bonding-enhanced format of the DREIDING (Mayo et al., 1990) force field was used. Five heating and cooling cycles were executed between 300 K and 800 K to maximize the system's density. After the last heating-cooling cycle, an isobaric NPT dynamics ensemble, with a Berendsen thermostat (100fs temperature damping factor), was applied for ten (10) ns, to guarantee thermal equilibrium and volume convergence.

The amorphous PMMA and nano-composite system were then deformed under uniaxial tensile strain applied at a constant strain rate ($10^6\ s^{-1}$) with a constant pressure condition for the two lateral cell faces. The polymeric system and two nanocomposites were deformed in multiple directions: x, y, and z. The average computed stress on x, y, and z directions were calculated. A local regression technique with an adjacent averaging model under Origin® software (OriginPro-7, 1991) was used to reduce fluctuations.

Size effects on the interactions between silica NPs and a poly (methyl methacrylate) or PMMA polymeric matrix were quantitatively evaluated through thermodynamic analysis of nanocomposite systems. Entropy (S), free-energy (G), and internal energy (E) were derived from relatively short molecular dynamics trajectories, using the two-phase thermodynamic method (2-PT) (Lin et al., 2003, 2010). In the following section,

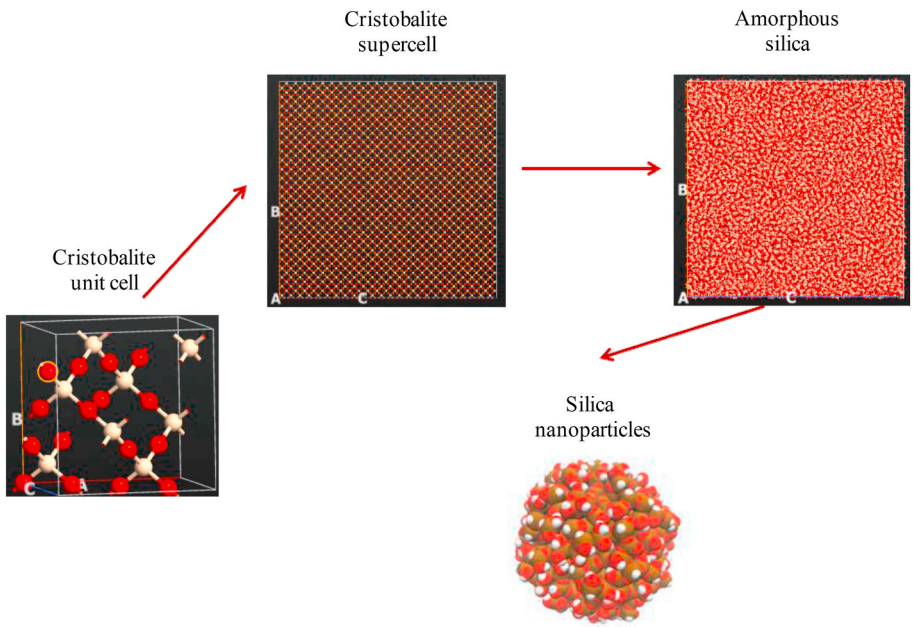

Fig. 1. Silica particle building process.

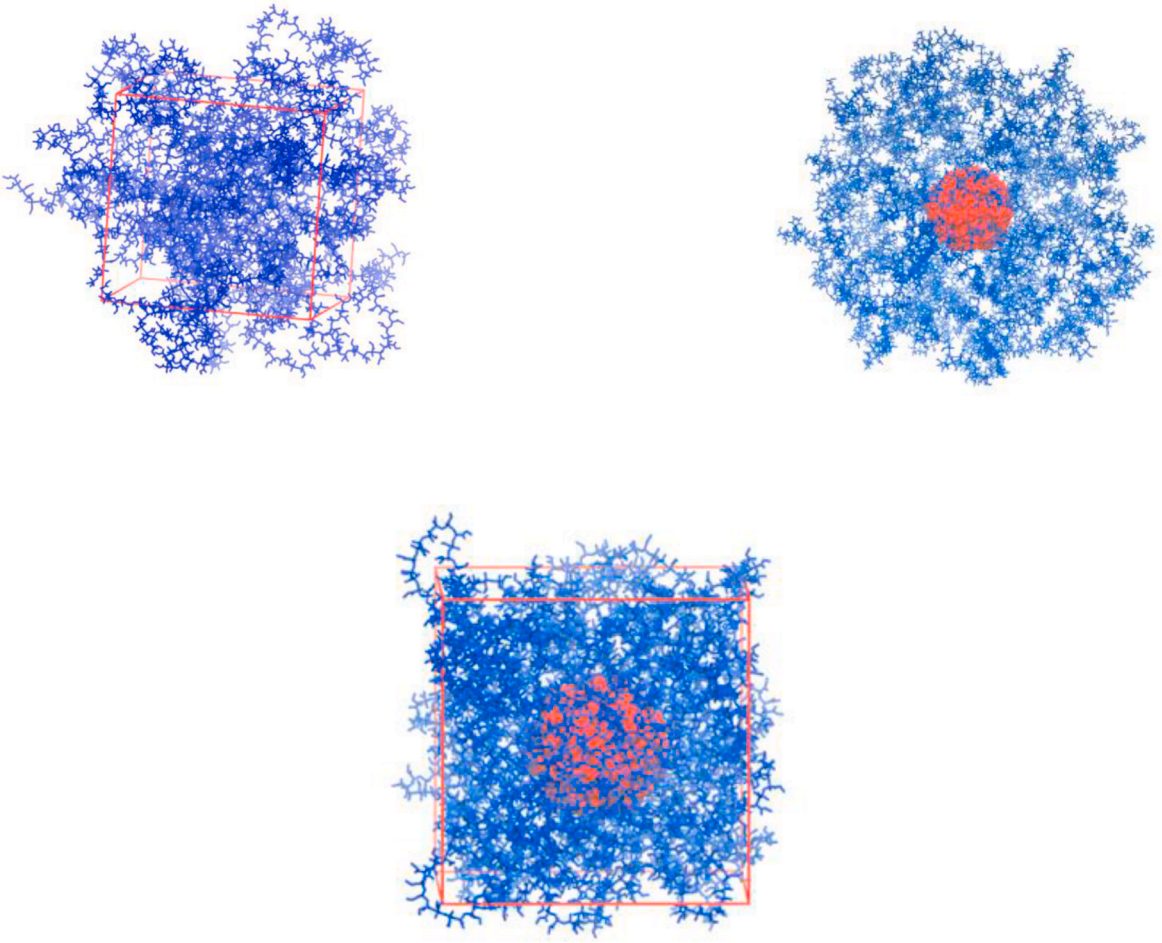

Fig. 2. Snapshot of the systems built; **top left**: polymer matrix made of 10 chains, each made of 200 monomers; **top right**: first construct of nano-composites made of 3 nm silica particles embedded into 10 chains of PMMA, each made of 200 monomers using Packmol software (Martínez and Martínez, 2003; Martínez et al., 2009); **bottom**: a nanocomposite system made of 3 nm particles embedded into twenty chains, each made of 200 monomers after equilibration under the LAMMPS molecular dynamics platform (http://lammps.san; Plimpton, 1995).

macroscopic mechanical results along with the interfacial interaction analysis will be presented and then discussed.

3. Results

3.1. ✓Macroscopic mechanical analysis

Fig. 3 illustrates the stress-strain response of the different systems. The presence of silica NPs induced an overall increase in the stiffness of the material compared to the polymer matrix alone.

The simulation used a general force field with a harmonic representation of bonded atom interaction; for this reason, it cannot describe covalent-driven failure, just hydrogen bond breaking. The overall mechanical response on larger strain domains could thus be used to qualitatively compare the mechanical behavior between the polymeric matrix and the binary systems. Only the elastic regime, however, could be used to deduce quantitative material properties. Fig. 4 presents the linear regime of the stress-strain curves of stretched systems. Linear fitting was used to help deduce the linear elastic modulus. The elastic modulus of the polymeric matrix determined from the slope of the linear regime was found to be 2.59 GPa, which is comparable with previous molecular dynamics results in the literature (Arash et al., 2014). For the composite material, the elastic modulus was found to be 7.67 GPa, while the 196% increase induced by the 3 nm NP compared to virgin PMMA. In comparaiso, the 4 nm NP composite system present en enhancement of the elastic modulus of 70% (elastic modulus about 4.41 GPa). The MD results are in the same advance with the previously obtained experimental data (Fig. 4) (Bliviet al., 2016; Blivi et al., 2020; Bedoui et al., 2012). Given the difference in the strain rate condition of MD simulations and experimental data, these results are only meant for ***qualitative*** comparison.

In the following section, the influence of the high surface-to-volume ratio on the interaction mechanisms at the silica-PMMA interface will be presented through quantitative thermodynamic properties.

3.2. ✓Interfacial interaction analysis

To analyze the thermodynamic properties of our system, we applied the two-phase thermodynamic method (2 PT) (Lin et al., 2003). From the density of state theory (Lin et al., 2003, 2010; Pascal et al., 2011), it is possible to derive local entropy and free energy at the scale of atoms, an ensemble of atoms, or molecular chains, by using individual or collective atomic velocities. At each MD step, the spectral density of the system could thus be determined from:

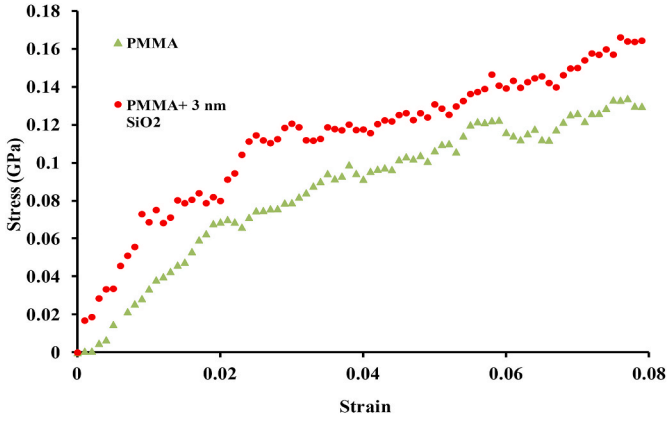

Fig. 3. Mechanical response of the polymeric matrix and composite system made with 3 nm silica NP.

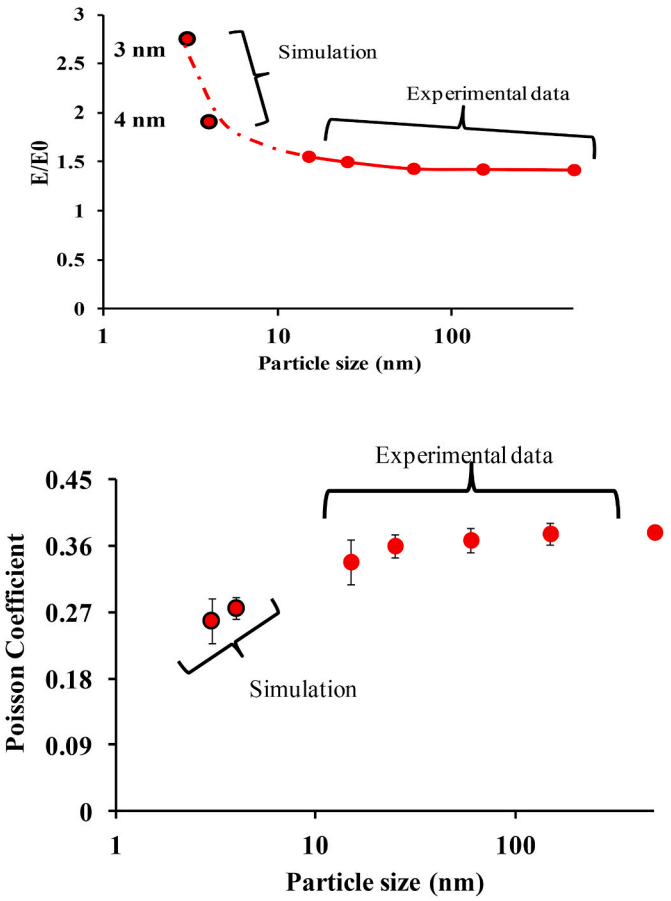

Fig. 4. Comparaison of the obtained Young modulus (**top**) and Poisson coefficient (**bottom**) with experimental data and additional 4 nm NP composite system.

$$s_j^k\left(\nu\right) = \lim_{\tau\to\infty}\left|\int_{-\tau}^{+\tau} V_j^k(t)\, e^{-i2\pi\nu t}dt\right|^2 \tag{1}$$

where V_j^k is the k component (x, y, or z) of the jth atom's velocity. Based on the work of Lin et al. (2003) the density of the states of the heterogeneous system is then derived as:

$$S(\nu) = \frac{2}{K\,T}\sum_{j=1}^{N}\sum_{k=1}^{3} m_j s_j^k(\nu) \tag{2}$$

where m_j is the mass of the atom j, and N is the total number of atoms in the system.

For solid systems, the normal modes are harmonic, hence from the density of states we can derive the canonical partition function Q:

$$Ln(Q) = \int_0^{\infty} d\nu S(\nu) Ln(q) \tag{3}$$

where $q = \dfrac{\exp\left(-\frac{\beta h\nu}{2}\right)}{1-\exp\left(-\frac{\beta h\nu}{2}\right)}$ with $\beta = 1/KT$ and h the Plank constant.

Integrating the density of states function according to Lin and Blanco (Lin et al., 2003) will lead to quantitative estimation of the thermodynamic properties (internal energy, entropy, and Helmholtz free energy) of the system, as follows:

$$E = E_0 + T\beta^{-1}\left(\frac{\partial Ln(Q)}{\partial T}\right)_{N,V} = E_0 + \beta^{-1}\int_0^{\infty} S(\nu)W_E(\nu)d\nu \quad (4)$$

$$S = KLn(Q) + \beta^{-1}\left(\frac{\partial Ln(Q)}{\partial T}\right)_{N,V} = K\int_0^{\infty} S(\nu)W_S(\nu)d\nu \quad (5)$$

$$A = E_0 - \beta^{-1}Ln(Q) = V_0 + \beta^{-1}\int_0^{\infty} S(\nu)W_A d\nu \quad (6)$$

where E_0 is the potential energy at $0^\circ K$ and W_E, W_S and W_A are the internal energy, entropy, and Helmholtz free energy weighting function, respectively, which can be expressed as:

$$W_E(\nu) = \frac{\beta h\nu}{2} + \frac{\beta h\nu}{\exp(\beta h\nu) - 1} \quad (7)$$

$$W_s(\nu) = \frac{\beta h\nu}{\exp(\beta h\nu) - 1} - Ln[1 - \exp(-\beta h\nu)] \quad (8)$$

$$W_A(\nu) = Ln\left[\frac{1 - \exp(\beta h\nu)}{\exp(-\beta h\nu)}\right] \quad (9)$$

This approach gives access to atom-based energy decomposition, based on atomic velocities, which can be extended to groups of atoms.

Here, we built atomic clusters to map the thermodynamic response to particular groups within the topological hierarchy of the heterogeneous systems considered. In other words, interfaces, and bulk ensembles, were used to determine the local energy decomposition for each topological level. To account for the interfacial properties, the PMMA matrix was decomposed into concentric layers of atoms from different polymer chains, but located at equal distances from the center of the mass of the silica NP (Fig. 5).

The entropy and internal energy distribution around the particles are given in Fig. 6. The closest layers, less than 10 Å from the silica NP, exhibit the most variation in both entropy and internal energy. While for the furthest layers, at more than 10 Å, both entropy and energy showed stable profiles. This can be explained by the fact that the closest layers are subject to strong silica surface-polymer interactions. In this region, we observed domains with fluctuating entropy and internal energy. Low entropy corresponds to high internal energy and *vice versa*. The lower the entropy, the more ordered the polymer packing, which in turn implies high interaction and thus high internal energy.

The internal energy and entropy variations were studied on the stretched system. Uniaxial tension was applied along X, Y, and Z at different strain levels within the proportionality region. When the strain level was reached (1–8%), a 20 ps trajectory under the NVT ensemble was dumped and post-processed to derive the entropy and internal

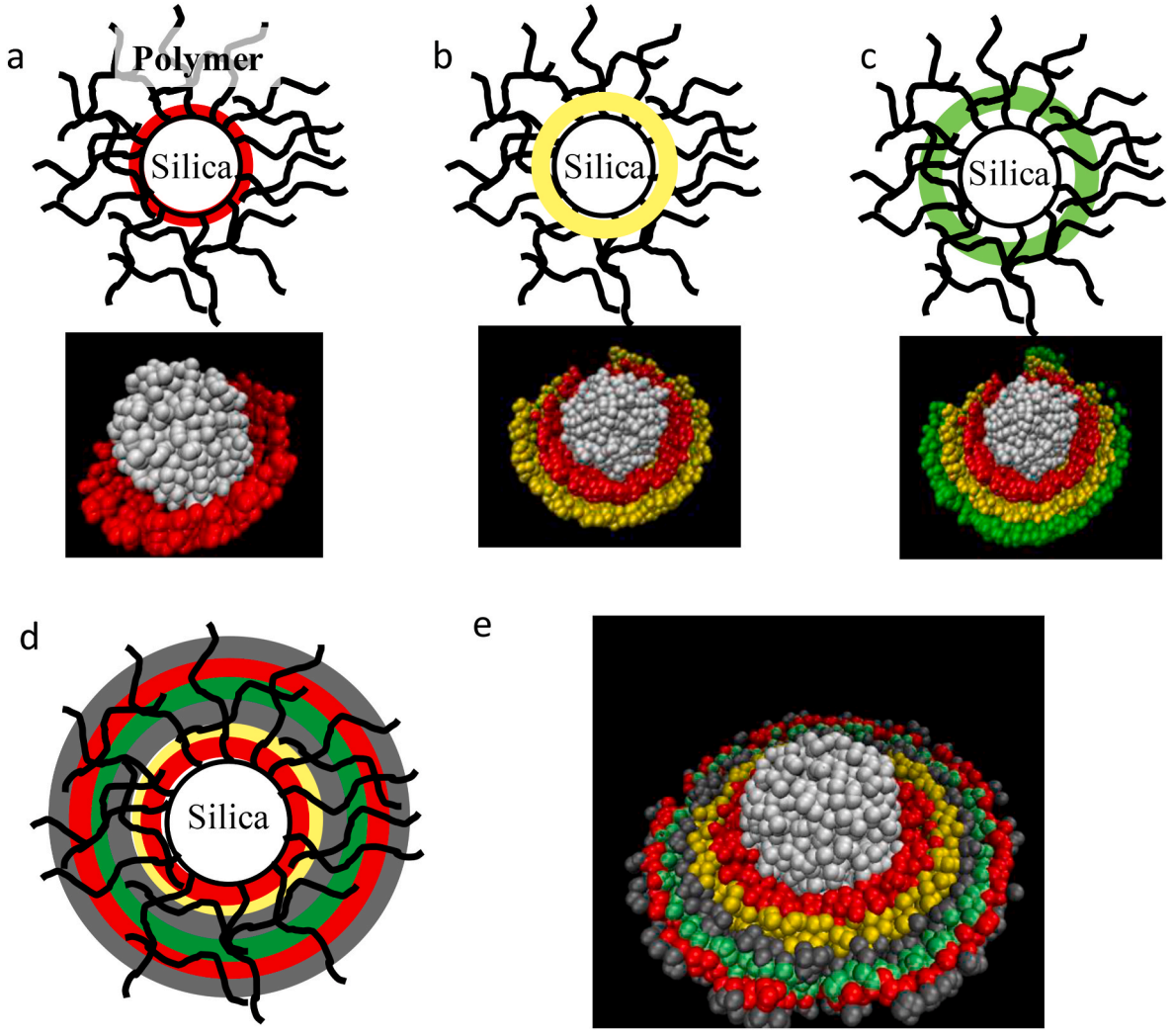

Fig. 5. Layer-by-layer system analysis; a), b) and c) layer identification, d) layer distribution diagram, e) silica NP and surrounding layers represented by the corresponding atomic van der Waals spheres.

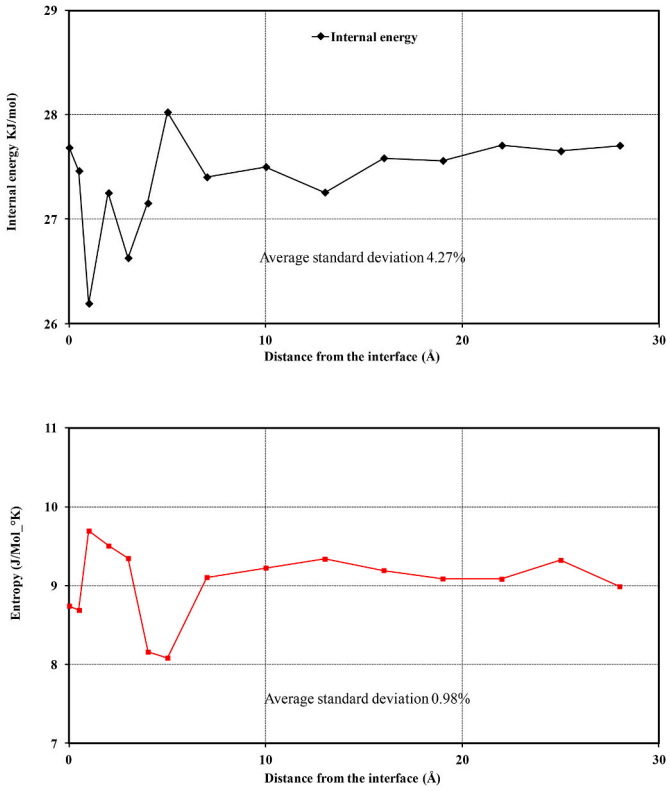

Fig. 6. Internal energy (top) and entropy (bottom) distribution: from the interface to the bulk-like matrix.

energy. For statistical consistency, five trajectories were processed for each strain level. The entropy and internal energy variations were calculated as the difference between two states; namely the stretched and initial states (unstrained sample). Fig. 7 represents the entropy and internal energy variations for the nanocomposite system throughout the polymer-silica interfacial layers. Two distinct domains could be identified through the entropy and internal energy variations: the polymeric layer within 1 nm of the silica surface, and the bulk-like polymer materials.

In the first domain, entropy and internal energy variations correlated with the applied strain. For stretching of less than 2%, there was no significant entropy variation compared to the internal energy variation. At this stretching level, the closest polymer layer seemed well ordered with no room left for chain re-conformation. For higher stretching levels, between 2 and 6%, both entropy and internal energy variations were noticed. The stretching induced a decrease in entropy vs an increase in internal energy. As such, the targeted layer underwent a reordering process. When it reached 8% stretching, internal energy decreased while entropy increased. This behavior could be interpreted as a decrease in interaction energy, leaving more opportunity for chain mobility to attain a new conformation at a low energy barrier.

For the second domain, while internal energy variations remained moderate, system entropy appeared to be more pronounced. In this region, polymeric behavior was a mostly conformation-change-driven process.

4. Discussion

The point of using a stiff inclusion in a soft matrix is to benefit from both the strength of the particles and their shape so the stretching-induced stress bypasses the soft matrix and can therefore be shared with the stiff embedded particle. In micromechanics, this is called the localization effect. This phenomenon is expressed through the localization tensor in micromechanics (Eshelby, 1957). As such, by increasing

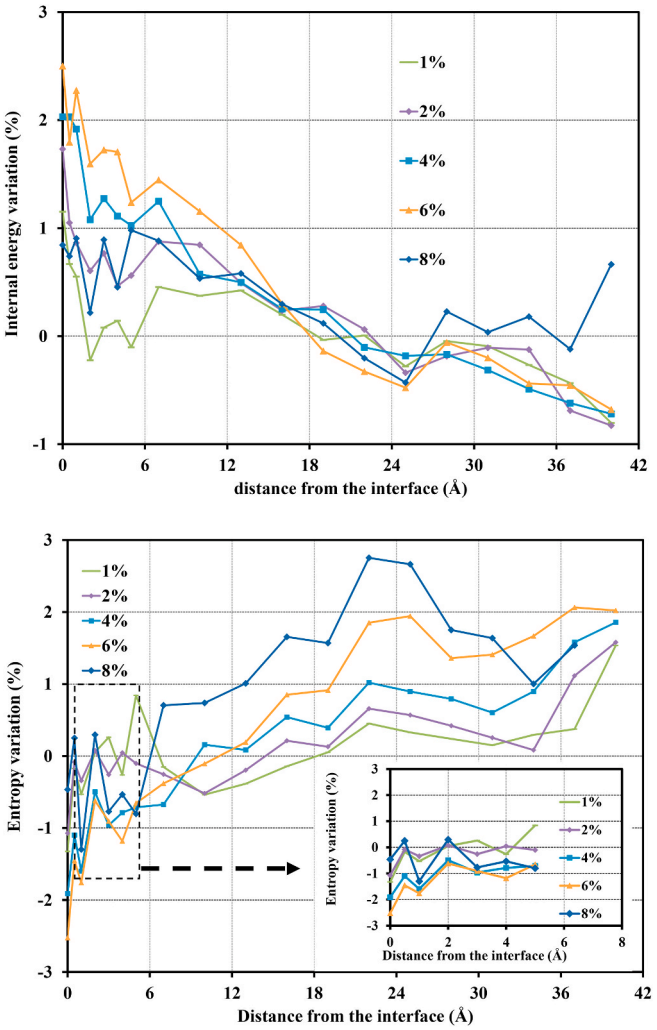

Fig. 7. Top: deformation-induced internal energy variations from the interface to the bulk-like material. Bottom: deformation-induced entropy variations from the interface to the bulk-like material.

the reinforcement particle volume fraction we explicitly increased the contact surface between the soft matrix and the stiff particles, which in turn induced stiffer composite materials. In our case, using 3 nm NP was an ideal configuration for a high surface-to-volume ratio and maintain a small system to simulate at low computing cost. For our silica particles, the surface-to-volume ratio for 3 nm diameter particles was equal to 2 nm^{-1}, whereas, for the same volume fraction, the same ratio for particles of 100 nm in size (as an example of larger NP embedded in the polymeric matrix) would be 0.06 nm^{-1}. The increase in surface-to-volume ratio while decreasing particle size explicitly induced an increase in particle surface compared to the system volume. The composite system was simulated as periodic boxes with side lengths of 6.6 nm, meaning the surface particle-to-box volume ratio was 9.4 10^{-2} nm^{-1}. In the equivalent system made of 100 nm NP, the same ratio would be 2.65 10^{-3} nm^{-1}. Compared to a nanocomposite system made of silica nanoparticles measuring 100 nm in diameter at the same volume fraction particle surface-to-system volume ratio would be 2.29 10^{-3} nm^{-1}. In this case, the 3 nm silica-based nanocomposite offers almost 30 times more surface-to-volume ratio.

The physical picture we can deduce from the previous results is that smaller particles offer a higher surface by which stress can bypass the soft matrix and therefore be supported by stiff particles. Hence, for a constant volume fraction, in addition to the particles' mechanical properties, the role played by particle surface is of paramount

importance. The high surface-to-volume ratio provided by nano-sized particles could be considered as a driving parameter in the enhancement of elastic properties.

Analyzing interfacial entropy for the nanocomposite systems revealed two effects of particle size on the entropy on the polymeric layers. In Fig. 8, entropy and internal energy variations were derived for each layer. During stretching, the first layers showed limited variations in entropy. The surface effect considered in the previous section as the parameter inducing overall stiffening of the composites also seemed to affect polymer ordering. The closest layers seemed well ordered and therefore showed high internal energy variations. The interfacial layer (less than 5 Å from the silica surface) exhibited the most pronounced variations in terms of entropy and internal energy. Also, it appears clearly that the decrease of 8% stretching was mostly governed by the interfacial interaction. The effects of the following layers seemed much milder.

Another point that should also be noted is mostly related to the contrast in internal energy variations for the composite and the matrix (see inset of Fig. 8-bottom). The overall response of the composite was nonlinear, whereas the matrix exhibited an almost linear response. This may suggest that the macroscopic nonlinearity observed was mostly an interfacial-driven phenomenon.

In our case, the silica surface was hydrogen-terminated to avoid any erroneous coordination of the surface oxygen atoms. The presence of the oxygen atom in the carbonyl and alkoxyl groups of the PMMA monomer side chain on the one hand, and the hydrogen termination of the silica on the other, was a condition that was favorable for the formation of hydrogen bonds. It could also be seen that the increased surface-to-volume ratio induced by small particles was a favorable context for hydrogen bonding, which in turn induced a more ordered structure at the interface. attractive interactions have been shown in previous works to be responsible for restricting polymer mobility (Rittigstein et al., 2007; Cheng et al., 2017; van Zanten et al., 1996) Although only hydrogen bonding interactions may occur at the surface between the PMMA and silica, this was enough to induce gradient segmental mobility on a large polymeric layer around the silica nanoparticle (Papon et al., 2011; Şerbescu and Saalwächter, 2009). This interaction decreases in perfect correlation with the stress increase induced by th stretching (Fig. 9).

The PMMA monomer has the advantage of having both oxygen atoms (carbonyl and alkoxyl groups) on the side chain. Both oxygen atoms are far from the polymer backbone making them less hindered sterically. Therefore carbonyl and alkoxy oxygen atoms may simultaneously interact with a single silanol group, making a joint hydrogen bond much stronger than a hydrogen bond with a single oxygen atom (Mortazavian et al., 2016). As observed in the work by Tang et al. (2017), the existence of interfacial hydrogen bonds effectively restricts the free movement of PMMA segments at the interface, thus increasing their thermal stability. The energy at the interface through the hydrogen bonding is an important constituent of the energy interaction as it

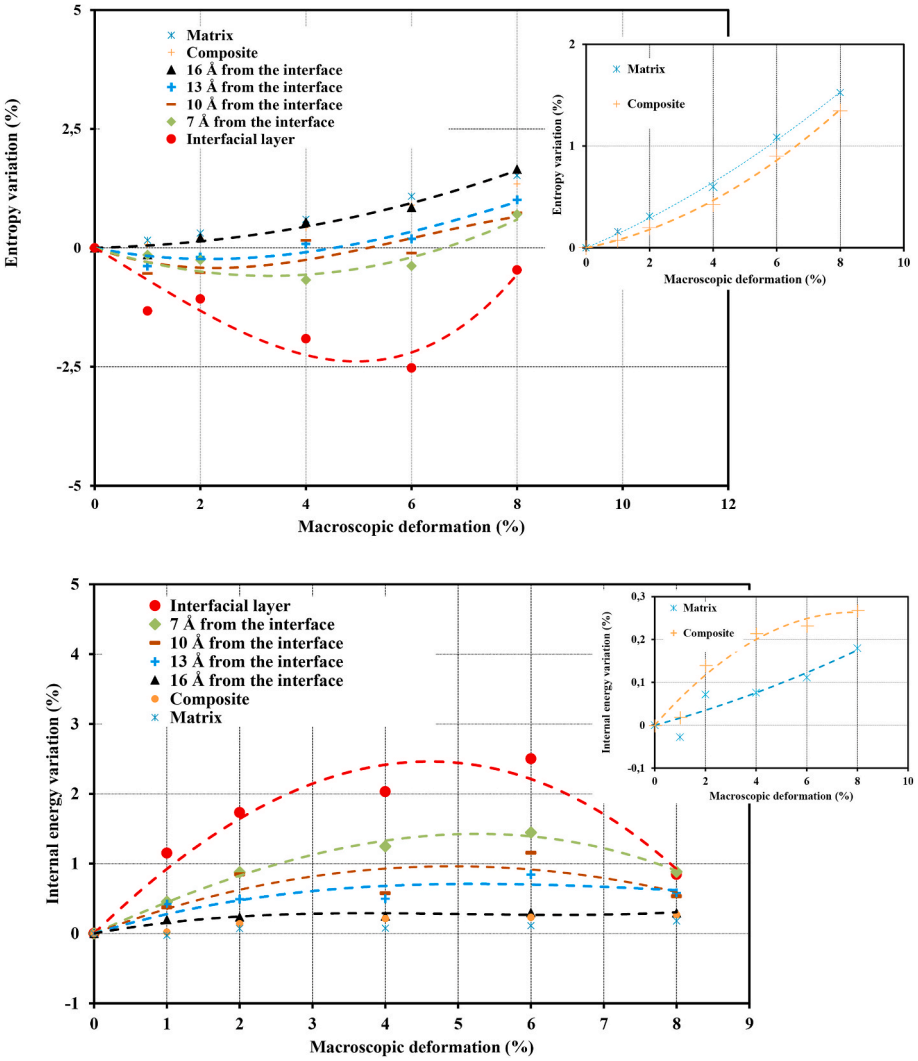

Fig. 8. Layer-by-layer entropy (top) and internal energy (bottom) variations. In both figures, the onsets represent the composite and matrix responses.

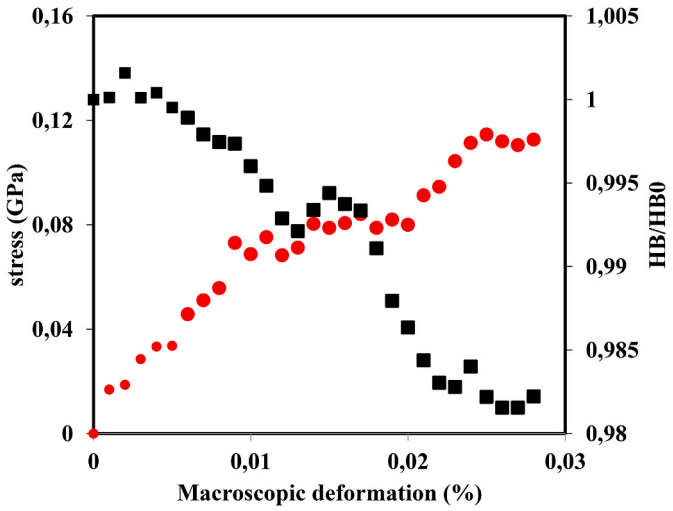

Fig. 9. Hydrogen bonding energy variation throughout the stretching path for the 3 nm-based composite.

promotes the interaction between PMMA and silica. It also induces what is called in the literature "tightly bound" segments (Mortazavian et al., 2016; Blow, 1973) or rigid amorphous phase (Wunderlich, 2003), which refers to the polymer segments bound to the silica surface through the hydrogen bonding mechanisms. Such interaction at the PMMA-silica interface is size-dependent (Tang et al., 2017). In a similar configuration made of silica particles embedded in a PMMA matrix (Tang et al., 2017), the energy density of the hydrogen bonding was enhanced in systems where the polymer chains were mixed with smaller silica nanoparticles (Tang et al., 2017). Such interactions in addition to tightly binding the PMMA chain to the silica particle, also seem to enhance inter-chain interaction by favoring the rigid amorphous phase around the silica NPs (Mortazavian et al., 2016).

As a result of the previous observations, the nanocomposite system showed a gradient of ordered layers from the interface to the bulk-like material. Within the first layers, the interplay between entropy and internal energy variations was noticed while stretching the sample. This type of phenomenon may be considered the consequence of the strong interaction between the silica surface and the surrounding polymeric chain. Favorable conditions for hydrogen bonding between the silica surface and the polymer chain also contribute to this observation.

The following polymer layers showed higher entropy variation, which could be interpreted as a deformation-induced disorder. The further the oxygen atom from the silica silanol groups, the less intense are the interactions, and consequently, the more mobile the polymeric chains. According to the work by Papon et al. (2012), this reflects the role played by the nanoparticle to induce mobility restriction in its vicinity and how this effect vanishes far from the interface as studied in previous works (Rittigstein et al., 2007; Papon et al., 2011, 2012; Cheng et al., 2017; van Zanten et al., 1996; Solar et al., 2017; Golitsyn et al., 2017). enhanced mobility within the polymeric chains away from the silica surface.

Our model accurately describes the interfacial interaction between nanoparticles and how they govern the deformation mechanisms. It helps correlate the interface interaction to the mechanical properties. This mechanism is at the heart of the experimentally observed mechanical enhancement of polymer matrices with silica nanoparticles. Based on these findings, mechanical modeling of nano-reinforced polymers may not be based on interfacial stress discontinuity or polymeric layers with different mechanical properties from the bulk matrix but should include both configurations for a better description of the overall mechanical response of such materials. Future studies targeting the change in thermodynamic properties as a function of temperature and stretching should help quantify the mechanical and physical properties of the interfacial polymeric matrix. Such results will be highly valuable for engineering studies of nano-reinforced polymers.

5. Conclusion

PMMA matrix behavior was compared to nano-reinforced composites with 3 nm embedded silica NPs. The composite system was investigated at different length scales, and we reported on the system's response to stretching, energy interactions at the interface, and quantified different thermodynamic regimes at the interface and within the polymeric bulk. The results derived from this study suggest that small nanoparticles induce ordered polymeric layers at the interface. As a result of the enhanced ordering at the interface, while stretching the samples, the interaction energy at the interface through the hydrogen bonds was better maintained, leading to higher mechanical properties.

The physical picture we can draw from this study on the advantages of reinforcing polymeric materials with stiff nanoparticles comes from three essential conditions: 1) good dispersion, 2) good affinity and 3) smaller particle size. When targeting nano-reinforced polymers, it is essential to achieve complete and homogenous dispersion of the filler into the matrix, to maximize the interfacial effects. Reducing particle size leads to an increase in the contribution of the well-ordered layers at the interface between the polymer and the NP. The affinity between particles and the surrounding polymeric matrix is a favorable condition for increasing interactions between nanoparticles and the surrounding matrix. This affinity is a bolstering parameter allowing the nanoparticles to fully express their interfacial area. In our case, the presence of oxygen atoms on the side chain (the carbonyl and alkoxyl groups) created a more favorable condition for hydrogen bonding interaction, leading to an enhanced locally ordered structure. As the induced order was size-dependent, the smaller particles thus induced a naturally higher interaction and a well-ordered interface, and therefore better mechanical properties.

Author statement

This paper was authored by: Fahmi Bedoui, Andres Jaramillo-Botero Tod A. Pascal an and William A. Goddard III.

Fahmi BEDOUI carried out the MD simulation. Andres Jaramillo Botero contributed to this work on advising on the MD simulation and the use of LAMMPS software. Tod A. Pascal assisted through his expertise on the use of the 2-T method. William A. Goddard contributed through his guidance on the wise use of the atomistic concepts and help revising the manuscript in its first format.

Data availability

The data that support the findings of this study are available from the corresponding author upon reasonable request.

Declaration of competing interest

The authors declare that they have no known competing financial interests or personal relationships that could have appeared to influence the work reported in this paper.

Acknowledgment

The authors would like to acknowledge the funding support from Région Hauts de France through the INTIM and SENAREO project (RDIPROJFT63 – INV 31) and the helpful support in the computing process from Guy Leon Kaza (Roberval Laboratory FRE-CNRS 2012) and Malik Abbassi (SAS Neoteckno). Caltech received support from DOE (STTR Award DE-SC0017710).

References

Arash, B., Wang, Q., Varadan, V.K., 2014. Mechanical properties of carbon nanotube/polymer composites. Sci. Rep. 4 (1–4), 6479.

Bedoui, F., et al., 2012. Anomalous increase in modulus upon hydration in random copolymers with hydrophobic segments and hydrophilic blocks. Soft Matter 8 (7), 2230–2236.

Berriot, J., et al., 2002. Evidence for the shift of the glass transition near the particles in silica-filled elastomers. Macromolecules 35 (26), 9756–9762.

Blivi, A.S., et al., 2020. Multiscale analysis of nanoparticles size effects on thermal, elastic, and viscoelastic properties of nano-reinforced polymers. Polym. Eng. Sci. 60 (8), 1773–1784.

Blivi, A.S., et al., 2016. Experimental evidence of size effect in nano-reinforced polymers: case of silica reinforced PMMA. Polym. Test. 56, 337–343.

Blow, C.M., 1973. Polymer/particulate filler interaction—the bound rubber phenomena. Polymer 14 (7), 309–323.

Brisard, S., Dormieux, L., Kondo, D., 2010. Hashin–Shtrikman bounds on the bulk modulus of a nanocomposite with spherical inclusions and interface effects. Comput. Mater. Sci. 48 (3), 589–596.

Brown, D., et al., 2008. Effect of filler particle size on the properties of model nanocomposites. Macromolecules 41 (4), 1499–1511.

Cheng, S., et al., 2017. Focus: structure and dynamics of the interfacial layer in polymer nanocomposites with attractive interactions. J. Chem. Phys. 146 (20), 203201 1–20320114.

Chevigny, C., et al., 2011. Tuning the mechanical properties in model nanocomposites: influence of the polymer-filler interfacial interactions. J. Polym. Sci. B Polym. Phys. 49 (11), 781–791.

Diani, J., Gilormini, P., 2014. Using a pattern-based homogenization scheme for modeling the linear viscoelasticity of nano-reinforced polymers with an interphase. J. Mech. Phys. Solid. 63, 51–61.

Dormieux, L., Kondo, D., 2013. Non linear homogenization approach of strength of nanoporous materials with interface effects. Int. J. Eng. Sci. 71, 102–110.

Eshelby, J.D., 1957. The determination of the elastic field of an ellipsoidal inclusion and related problem. Proc. Roy. Soc. Lond. 241 (A), 376–396.

Golitsyn, Y., Schneider, G.J., Saalwächter, K., 2017. Reduced-mobility layers with high internal mobility in poly(ethylene oxide)–silica nanocomposites. J. Chem. Phys. 146, 1–8, 203303.

LAMMPS, http://lammps.sandia.gov.

Lin, S.-T., Blanco, M., Goddard, W.A., 2003. The two-phase model for calculating thermodynamic properties of liquids from molecular dynamics: validation for the phase diagram of Lennard-Jones fluids. J. Chem. Phys. 119 (22), 11792–11805.

Lin, S.-T., Maiti, P.K., Goddard, W.A., 2010. Two-phase thermodynamic model for efficient and accurate absolute entropy of water from molecular dynamics simulations. J. Phys. Chem. B 114 (24), 8191–8198.

Lucchetta, A., Brach, S., Kondo, D., 2021. Effects of particles size on the overall strength of nanocomposites: molecular Dynamics simulations and theoretical modeling. Mech. Res. Commun. 103669.

Marcadon, V., Herve, E., Zaoui, A., 2007. Micromechanical modeling of packing and size effects in particulate composites. Int. J. Solid Struct. 44 (25), 8213–8228.

Martínez, J.M., Martínez, L., 2003. Packing optimization for automated generation of complex system's initial configurations for molecular dynamics and docking. J. Comput. Chem. 24 (7), 819–825.

Martínez, L., et al., 2009. Packmol: a package for building initial configurations for molecular dynamics simulations. J. Comput. Chem. 30 (13), 2157–2164.

Matestro, 2018. Schrödinger Release 2018-3. Maestro, Schrödinger, LLC, New York, NY.

Mayo, S.L., Olafson, B.D., Goddard, W.A., 1990. DREIDING: a generic force field for molecular simulations. J. Phys. Chem. 94 (26), 8897–8909.

Mortazavian, H., Fennell, C.J., Blum, F.D., 2016. Surface bonding is stronger for poly (methyl methacrylate) than for poly(vinyl acetate). Macromolecules 49 (11), 4211–4219.

OriginPro-7, SR0 OriginLab corporation. Copyright® . Northampton. 1991-2002.

Papon, A., et al., 2011. Low-field NMR investigations of nanocomposites: polymer dynamics and network effects. Macromolecules 44 (4), 913–922.

Papon, A., et al., 2012. Glass-Transition temperature gradient in nanocomposites: evidence from nuclear magnetic resonance and differential scanning calorimetry. Phys. Rev. Lett. 108 (6), 065702-1 065702-5.

Pascal, T.A., Lin, S.T., III, W.A.G., 2011. Thermodynamics of liquids: standard molar entropies and heat capacities of common solvents from 2PT molecular dynamics. Phys. Chem. Chem. Phys. 13 (1), 169–181.

Pascal, T.A., Lin, S.-T., Goddard Iii, W.A., 2011. Thermodynamics of liquids: standard molar entropies and heat capacities of common solvents from 2PT molecular dynamics. Phys. Chem. Chem. Phys. 13 (1), 169–181.

Pedone, A., et al., 2008. FFSiOH: a new force field for silica polymorphs and their hydroxylated surfaces based on periodic B3LYP calculations. Chem. Mater. 20 (7), 2522–2531.

Plimpton, S., 1995. Fast parallel algorithms for short-range molecular dynamics. J. Comput. Phys. 117 (1), 1–19.

Rittigstein, P., et al., 2007. Model polymer nanocomposites provide an understanding of confinement effects in real nanocomposites. Nat. Mater. 6, 278–282.

Ronald, E.M., Vijay, B.S., 2000. Size-dependent elastic properties of nanosized structural elements. Nanotechnology 11 (3), 139–147.

Schadler, L., 2007. Model interfaces. Nat. Mater. 6, 257–258.

Şerbescu, A., Saalwächter, K., 2009. Particle-induced network formation in linear PDMS filled with silica. Polymer 50 (23), 5434–5442.

Solar, M., Binder, K., Paul, W., 2017. Relaxation processes and glass transition of confined polymer melts: a molecular dynamics simulation of 1,4-polybutadiene between graphite walls. J. Chem. Phys. 146, 1–13, 203308.

Tang, C., Li, X., Hao, J., 2017. Interfacial hydrogen bonds and their influence mechanism on increasing the thermal stability of nano-SiO2-modified meta-aramid fibres. Polymers 9 (504), 1–18.

van Zanten, J.H., Wallace, W.E., Wu, W.-l., 1996. Effect of strongly favorable substrate interactions on the thermal properties of ultrathin polymer films. Phys. Rev. 53 (3), 2053–2056.

Wunderlich, B., 2003. Reversible crystallization and the rigid–amorphous phase in semicrystalline macromolecules. Prog. Polym. Sci. 28 (3), 383–450.

Yvonnet, J., Quang, H.L., He, Q.C., 2008. An XFEM/level set approach to modelling surface/interface effects and to computing the size-dependent effective properties of nanocomposites. Comput. Mech. 42 (1), 119–131.